

SODA LIME SILICATE GLASSES CONTAINING IRON OXIDE - IN VITRO EVALUATION

Irena Mihailova, Ruzha Harizanova, Nikoleta Shtapleva-Dimova,
Hristo Georgiev, Milena Nedkova-Shtipska

University of Chemical Technology and Metallurgy,
8 Kliment Ohridski Blvd., Sofia 1797, Bulgaria
E-mail: irena@uctm.edu

Received 01 November 2023

Accepted 01 September 2024

DOI: 10.59957/jctm.v59.i6.2024.10

ABSTRACT

Three glasses with different iron oxide concentrations (between 5 and 8.1 mol %) were obtained in the CaO - Na₂O - SiO₂ - Fe₂O₃ system by using conventional melting-quenching technique. The amorphous nature of the synthesized materials is confirmed by X-ray diffraction analysis, XRD. The physico-chemical and structural characterization of the glasses was performed by measuring their density, refractive indices, as well as by calculating the molar volume, oxygen packing density and recording the infrared spectra by Fourier Transformed Infrared Spectroscopy, FT-IR, respectively. The glasses were evaluated in vitro by examining bone-like apatite formation on their surfaces in a simulated body fluid, SBF. The structural changes in the glasses during the in-vitro test were traced by means of FT-IR and Scanning Electron Microscopy, SEM. The solutions were examined by Inductively Coupled Plasma Optical Emission Spectroscopy, ICP-OES to determine the ion exchange between the glasses and the starting SBF and the corresponding effect on the pH was also recorded.

Keywords: iron oxides, soda lime silica glasses, structure, in vitro bioactivity, hyperthermia biomaterials.

INTRODUCTION

The interest in the synthesis of magnetic materials is determined by their potential for various applications in the field of biomedicine. In the recent years multiple works concerning applications of magnetic materials such as magnetic hyperthermia [1, 2], drug delivery [2 - 4], magnetic resonance imaging, magnetic stimulation, bacterial detection and separation, diagnosis and treatment of infections have been published [5 - 10]. Though magnetite, Fe₃O₄ is supposed to be biocompatible, the application of iron oxide especially in case of nano-sized objects in biomedicine faces numerous risks as shown in the investigation of their in vitro/in vivo toxicity evaluation and quantification [11 - 14]. Magnetic glasses and glass-ceramics are alternative materials for bone cancer therapy by utilizing the method of hyperthermia [15]. The method is based on the idea that the cancer cells are more vulnerable and easier to destroy at elevated temperatures between 39 and 45°C

compared to the normal cells. By situating the glass-ceramics in the vicinity of the tumor and applying an alternative magnetic field, heat is generated due to the magnetic hysteresis loss [16]. It is established that there is a synergistic effect while combining hyperthermia and radiotherapy and chemotherapy, as the sensitivity of the cancer cells is increased.

Glass-ceramics are materials which can combine magnetic properties with biological activity, as their action is not solely associated to the destruction of the tumor formations but also should assist the regeneration of the damaged bone tissue. New research data show that the bioactive glass-ceramics could also assist the regeneration of soft tissues, and this opens new perspectives for the investigation and their application in biomedicine [15].

For several decades various glasses and glass-ceramics have been developed and investigated as application for cancer treatment by hyperthermia. After Kokubo has shown for the first time that it is possible

to combine magnetic and bioactive properties in one and the same material [17], several investigations have been carried out in the system CaO-SiO-Fe₂O₃ [18 - 21]. Highly desired crystalline phases which ensure the magnetic properties of the prepared materials are magnetite, Fe₃O₄ and maghemite, γ -Fe₂O₃. Regarding the optimization of the magnetic properties and the bioactivity of the glass-ceramics, more complicated as composition systems have been investigated, including Na₂O, Li₂O, MgO, ZnO, B₂O₃, P₂O₅, TiO₂, etc. [22 - 25]. Additionally, to the variation of the composition, also various synthesis techniques have been applied as for example: melt-quenching and controlled crystallization from the obtained glass [26, 27], melting the coprecipitation-derived precursors [28], modified solid-state sintering method [29], melt-quenching method using oxy-acetylene flame [30], sol-gel synthesis [21, 31 - 33]. The approach utilized in these investigations is by controlling the composition and tailoring the synthesis conditions to achieve a precise control over the phase composition and the structure of the prepared materials thus aiming to achieve the desired properties. The survey of the publications in which the ability of materials to accumulate on their surface apatite-like layer while being immersed in a simulated body fluid, SBF has been experimentally proven shows that in the composition of these materials bioactive crystalline phases such as wollastonite [21, 30, 33], hydroxyapatite [21, 30], other calcium and calcium-sodium silicates are present or that these materials are based on the classical compositions of bioglasses [34, 35]. Typical for the phase composition of glass-ceramics is the presence of an amorphous part as the main phase. In the composition of most of the magnetic glass-ceramics, iron oxides are one of the main constituents in the composition. There are, however, only few studies in which the biocompatibility and bioactivity of such glasses and derived from them glass-ceramics are investigated [19], though it is of great importance to elucidate the role of each component from the composition in these materials respectively if this constituent contributes to and stimulates the bioactive properties of the material. The development of glass-ceramics for biological implants requires precise control and thorough investigation of all crystalline and amorphous phases from which the respective material is composed.

Subject of the present investigation are the glasses

in the system Na₂O - CaO - SiO₂ - Fe₂O₃ with different concentrations of iron oxide prepared by applying a traditional melting method, which consists of quenching the melt from 1400°C. This is one of the systems in which magnetic bioceramics have been synthesized [33]. The molar ratios Na₂O:CaO:SiO are chosen to be close to that for the classical soda lime silica (window) glass. Ferrimagnetic bioactive glass-ceramic has been fabricated using soda lime silica waste glass as the main raw material but its composition was modified according to the Bioglasss 45S5 composition [24]. The goal of the current investigation is to monitor and evaluate the performance of the glasses in SBF as well as their *in vitro* bioactivity. For this reason, the glasses have been subjected to a static *in-vitro* test in SBF for 4, 7, 14 and 28 days. By applying several analytical techniques, the interaction of the material with the SBF solution has been traced. The samples obtained after the immersion in the SBF are subjected to an investigation by Fourier Transformed Infrared Spectroscopy, Scanning Electron Microscopy and Energy Dispersive X-Ray Spectroscopy. The pH values of the respective SBF solutions after the contact with the Fe-containing glasses have been measured and the changes in their composition have been registered by using the ICP-OES technique.

EXPERIMENTAL

Synthesis of the glasses

Tree glasses in the system Na₂O - CaO - SiO₂ - Fe₂O₃ were synthesized. The following reagent grade raw materials were used: Na₂CO₃, CaCO₃, SiO₂ and FeC₂O₄·2H₂O. The chemical compositions (in mol %) of the glasses are shown in Table 1. 2 wt. % carbon were added to the batch for the 5 mol % iron oxide glass to further reduce the iron. The glasses were prepared by melting in a fused silica crucible at a temperature of 1400°C in air for 1.5 h. After pouring into a pre-heated graphite-mould and after solidifying of the surface, the melts were transferred to a muffle furnace and annealed for 10 min at 480°C. Then the furnace was switched off and cooled to room temperature.

Characterization methods

The density of the samples was measured by utilizing the Archimedes principle, using an analytical scale Mettler Toledo New Classic ME 104 equipped with

a density determination kit for solids using distilled water as the immersion liquid. The Becke line method was used to determine the refractive indices of the synthesized glasses [36]. A small amount of powder from the studied sample was immersed in a liquid of a known refractive index and viewed through the microscope. A bright line, known as the Becke line, separates substances of different refractive indices. When the refractive indices of the glass and the immersion liquid are equal, the Becke line disappears. Thus, by successive application of different liquids with known refractive indices, the glass refractive indices were estimated. The refractive indices of the immersion liquids were always measured before the evaluation of the glass refractive indices by the Becke line method by an Abbe refractometer (Carl Zeiss Jena).

X-ray powder diffraction analysis, XRD was applied for phase control. An X-ray diffractometer Philips with Cu-K α radiation was used and a range from 7.5° to 95° 2 θ (step size: 0.05°, counting time per step: 1 s. Fourier Transformed Infrared Spectroscopy, FT-IR was utilized for the structural characterization of the samples and for recording possible changes in the phase composition after the *in vitro* test. The transmittance spectra of the samples were recorded by using the pressed-pellet technique in KBr. The measurements were performed by a FT-IR spectrophotometer Varian 660 IR in the frequency range from 4000 to 400 cm $^{-1}$.

The apatite forming ability of the synthesized glasses was assessed by immersion of the glass powders for 4, 7, 14 and 28 days in a Simulated Body Fluid, SBF prepared as described by Kokubo et al. [37]. 0.7 g of glass powder with a particle size of less than 100 μm was placed in plastic containers containing 40 ml of SBF at 37 \pm 0.5°C. When the samples were removed from the SBF solution by filtering, they were rinsed with ethanol and distilled water, dried and stored in

containers. After the immersion in SBF, the specimens were characterized by FT-IR. Particle surfaces, before and after the immersion in SBF, were examined by Scanning Electron Microscopy, SEM. Microscopic observations were carried out with a SEM/FIB LYRA I XMU microscope (TESCAN) equipped with an Energy Dispersive X-ray Spectroscopy, EDX analyzer. An EDX Quantax 200 (Bruker) detector was used to record the EDX spectra. The change of the concentrations of Ca, P, Si, Na and Fe in the SBF solutions as a result of the *in vitro* test was determined by Inductively Coupled Plasma Optic Emission Spectrometry, ICP-OES (Prodigy High Dispersion ICP-OES Spectrometer from Teledyne Leeman Labs). The pH values of the SBF solutions after contact with the iron-containing glasses were measured.

RESULTS AND DISCUSSION

Physico-chemical characterization

In Table 1, the information about the chemical composition, density, molar mass, molar volume, oxygen packing density and refractive index of the glasses is shown.

Two of the compositions are similar as far as the chemical compositions and the iron oxide concentrations are concerned but are prepared by using different synthesis conditions. The third composition has a relatively higher iron oxide concentration. The differences in the densities of the two samples with about 5 mol % Fe $_2$ O $_3$ witness for the occurrence of some structural differences between them as well as between them and the samples obtained in earlier studies [39]. The currently synthesized and investigated glasses have a lower density and lower refractive index. It could be suggested that the different redox-ratios for the iron ions present is the reason for this difference because depending on their valence and coordination, Fe-ions can

Table 1. Chemical composition, density, ρ , molar mass, M , molar volume, V_m , oxygen packing density, OPD and refractive index, n_0 of the glasses.

Compositions, mol %				ρ , g cm $^{-3}$	M , g mol $^{-1}$	V_m , cm 3 mol $^{-1}$	OPD, mol cm $^{-3}$	n_0
Fe $_2$ O $_3$	Na $_2$ O	CaO	SiO $_2$					
5	16	10	69	2.628	64.97	24.72	72.41	1.556
5.3	16.8	10.5	67.4	2.590	65.26	25.19	70.66	1.559
8.1	14.7	9.4	67.8	2.723	68.05	24.99	73.63	1.586

have different structural role in glass network. Thus, it could be concluded that the use of different raw materials for the iron oxide will result in different redox-ratios, i.e. different numbers of ferric and ferrous ions and this will lead to a different structure of the obtained glasses. The molar volume values for the investigated glasses are close to each other and are higher than those reported for other glasses with similar compositions [38]. One possible reason for this could be the higher number of ferrous ions in the present glasses which are known to be present in six-fold coordination in silicate glasses and serve as network modifiers, i.e. should lead to decreasing network connectivity and increasing V_m values. The OPD is highest for the glass with 8.1 mol % Fe_2O_3 , which corresponds to the increasing number of the oxygen ions for this glass with the increasing concentration of Fe_2O_3 . The refractive index values for the three glasses also increase with the increasing Fe_2O_3 concentration.

Structural characterization and *in vitro* bioactivity evaluation

The synthesized specimens are with dark coloration, macroscopically and microscopically homogenous, according to the performed optical microscopy inspection, with a sea shell-like fractured surface typical for glassy materials. The amorphous nature of the prepared materials is confirmed by the XRD analyses. In Fig. 1 the XRD pattern of glass with 5 mol % Fe_2O_3 is shown in which the typical amorphous halo and lack of diffraction peaks is observed.

In Figs. 2, 3 and 4 the FT-IR spectra of the starting (untreated) glasses as well as the spectra of the samples after the performed *in vitro* bioactivity tests in SBF are shown. All the spectra are typical for amorphous materials and consist of a small number of broad absorption bands.

In the FT-IR spectra of the untreated glasses, 3 main absorption peaks are observed in the spectral region between 400 and 1200 cm^{-1} which are characteristic for silicates. The most intensive absorption band is with a maximum at about 1014 - 986 cm^{-1} . It is asymmetric with shoulders at 1200 cm^{-1} and at approximately 900 cm^{-1} . Another intensive band is registered at about 463 - 454 cm^{-1} , and a band of smaller intensity - at 770 cm^{-1} . A shoulder in the spectra which is better expressed for the sample with the higher Fe-oxide concentration of 8.1 mol % Fe_2O_3 is detected at 690 cm^{-1} .

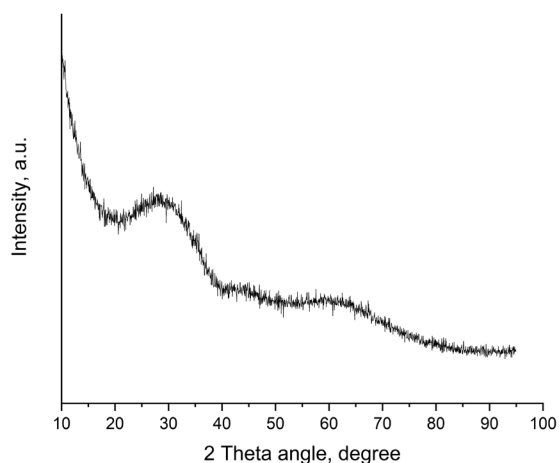


Fig. 1. XRD pattern of glass with 5 mol % Fe_2O_3 .

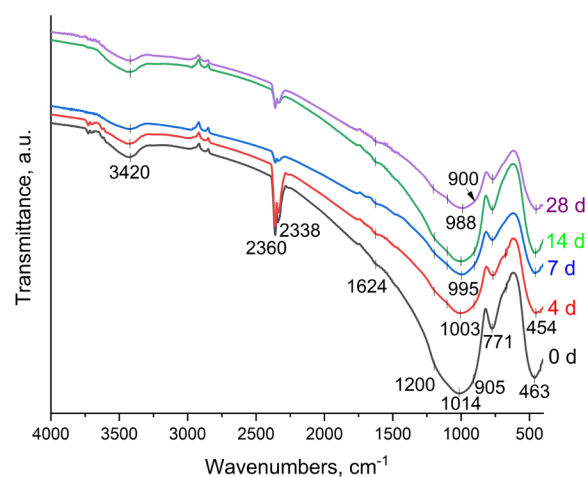


Fig. 2. FT-IR spectra of the glass samples with 5 mol % Fe_2O_3 before and after SBF tests (0 d - untreated glass, 4 d, 7 d, 14 d, 28 d - samples obtained after the immersion in a SBF for 4, 7, 14 and 28 days, respectively).

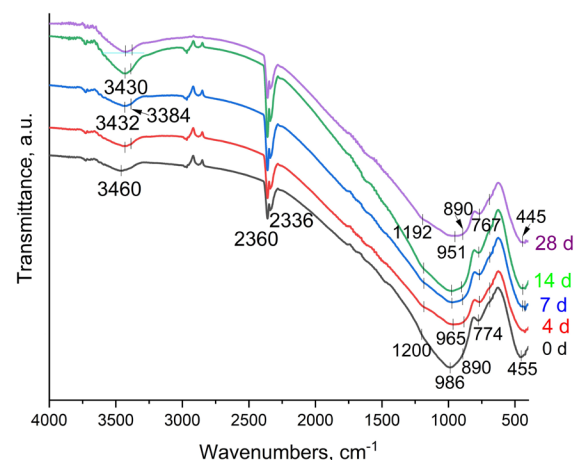


Fig. 3. FT-IR spectra of the glass samples with 5.3 mol % Fe_2O_3 before and after the SBF test (0 d - untreated glass, 4 d, 7 d, 14 d, 28 d - samples obtained after the immersion in a SBF for 4, 7, 14 and 28 days, respectively).

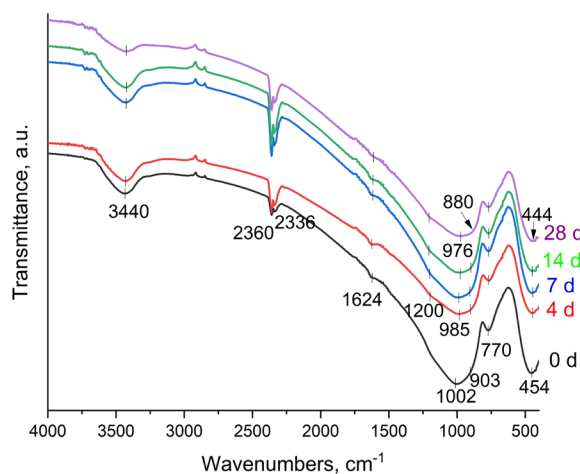


Fig. 4. FT-IR spectra of the glass samples with 8.1 mol % Fe_2O_3 before and after the SBF test (0 d - untreated glass, 4 d, 7 d, 14 d, 28 d - samples obtained after the immersion in a SBF for 4, 7, 14 and 28 days, respectively).

The bands between 1200 and 850 cm^{-1} can be ascribed to the asymmetric stretching vibration $\nu_d^{\text{as}}(\text{F})$ of the Si-O tetrahedra (SiO_4) [39]. According to the survey of numerous investigations performed, the position of this band depends on the degree of connectivity of the silicate network [39 - 41]. With Q^n , where $n = 0, 1, 2, 3$ and 4, the SiO_4 tetrahedra are designated depending on the number of bridging oxygens (BO). For example, Q^0 is an isolated tetrahedron and Q^4 is a tetrahedron sharing all its 4 oxygen ions with other tetrahedra. The change of the position of the maximum of this band from 1014 to 986 cm^{-1} in the initial (untreated) glasses could be attributed to the increasing degree of depolymerization of the glass network with the increasing concentration of Fe_2O_3 in the composition of the glasses. The prevailing structural units present in the three glasses are Q^2 , but the width as well as the asymmetry of the bands and the width of the shoulders at about 1200 cm^{-1} , 1100 cm^{-1} and 900 cm^{-1} witnesses also the presence of Q^4 , Q^3 and Q^1 structural units.

The band at 770 cm^{-1} , could be assigned to the symmetric bending modes of Si-O-Si bridges $\nu_d^{\text{s}}(\text{A})$, [39, 41]. The bands at 463 - 454 cm^{-1} are attributed to the bending vibration $\delta_d^{\text{as}}(\text{E})$ of Si-O-Si bridges [42]. In addition, the shoulder at 690 cm^{-1} could be most probably assigned to the occurrence of Fe-O stretching vibrations of four-fold coordinated Fe ions [38].

The FT-IR spectra of the samples obtained after

the immersion in a SBF for 4, 7, 14 and 28 days for each of the three studied compositions show changes, which can be attributed to the shift of the maxima of the main absorption bands, already, discussed above, to the lower wavenumbers and to a decrease of the respective intensities. In the contours of the compound asymmetric band between 1200 and 850 cm^{-1} , an increase in the absorption is established at about 900 cm^{-1} . On the other hand, no new bands appear in the FT-IR spectra which could be ascribed to the occurrence of calcium phosphates, and which could have witnessed the growth of an apatite layer at the contact surface of the samples. The characteristic lines of the carbonate group are also not established. Consequently, though certain structural changes occur in the iron-containing soda lime silicate glasses after the immersion and interaction with the SBF, these glasses do not demonstrate the ability to build an apatite-like layer on their contact surface for immersion periods of up to 28 days. This allows to conclude that, according to the experimental results obtained, the studied samples are not *in vitro* bioactive. According to previous research conducted by Ebisawa and Kokubo [43], it is considered that Fe_2O_3 -containing CaO - SiO_2 glass does not bond to living bone. Later the same authors found that bioactive glass-ceramics could be obtained from Fe_2O_3 -containing CaO - SiO_2 glasses with Na_2O , B_2O_3 and/or P_2O_5 added [19]. Therefore, the addition of sodium oxide positively affects the ability to bind to bone only for certain glass compositions in the system $\text{Na}_2\text{O} - \text{CaO} - \text{SiO}_2 - \text{Fe}_2\text{O}_3$.

The microphotographs shown in Fig. 5, illustrate the surface morphology of the glass containing 5 mol % Fe_2O_3 , before the immersion in SBF and after the performed *in vitro* bioactivity tests in the SBF with different duration - 4, 7, 14 and 28 days. The microscopic observations were combined with EDX-analyses of the contact surface of the investigated glasses with the SBF solution. The comparison of the batch compositions of the studied glasses with the ones obtained from the elemental analyses is given in Table 2. The data comparison shows a good coincidence. Some deviation is observed in the registered quantity for Si in the glasses, which is lower. During the performed analyses, either the absence of phosphorous or P quantities less than 1 wt. % are detected. Though in some regions at the surface of the samples treated in SBF for 14 and 28 days certain formations could be observed, cf. Figs. 5d - g, these formations do

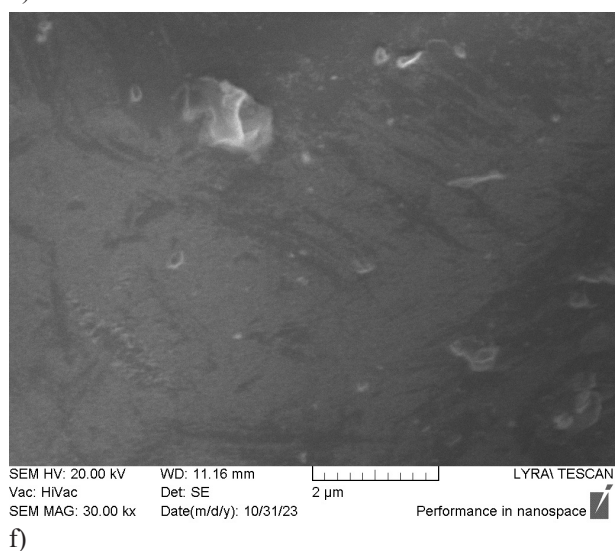
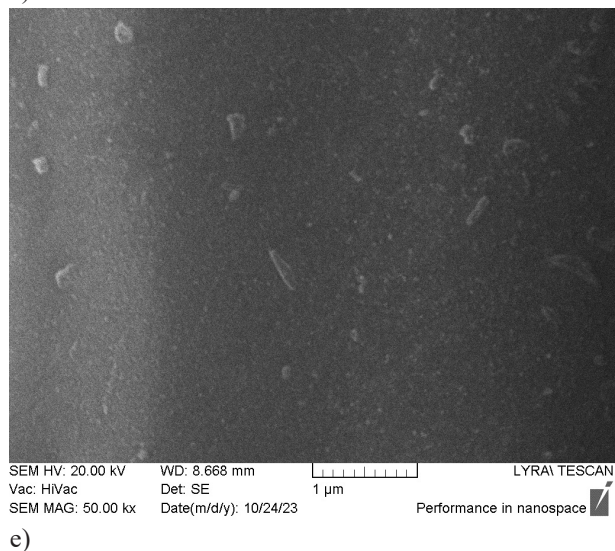
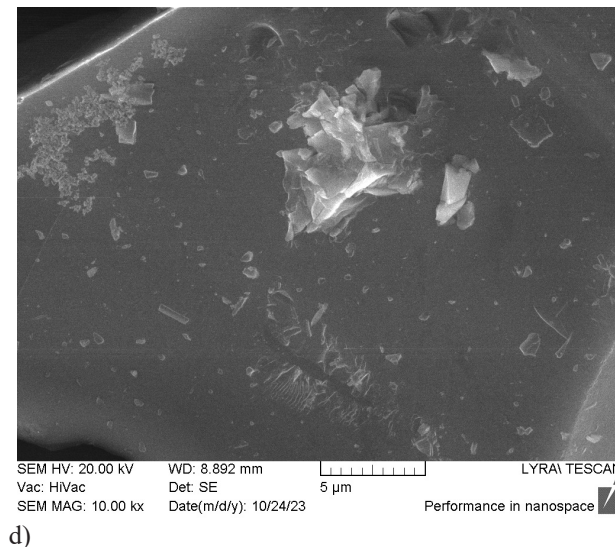
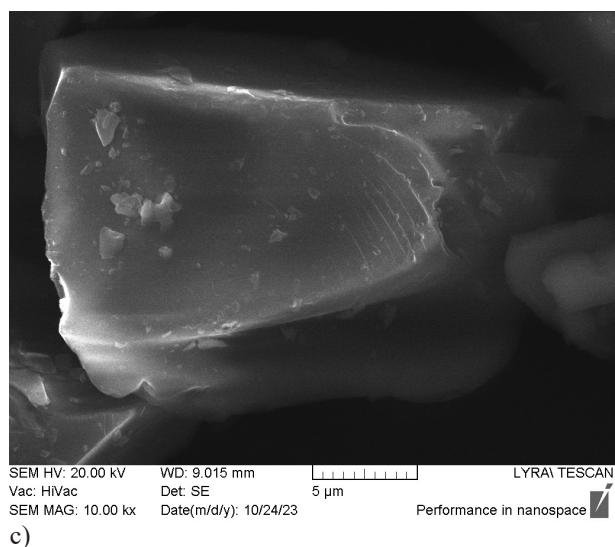
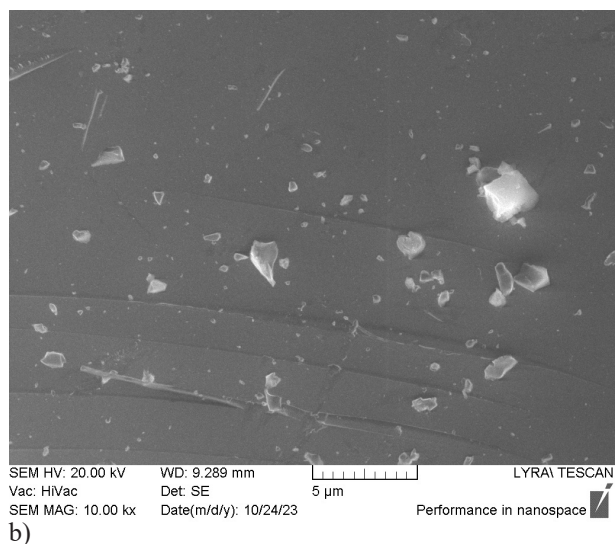
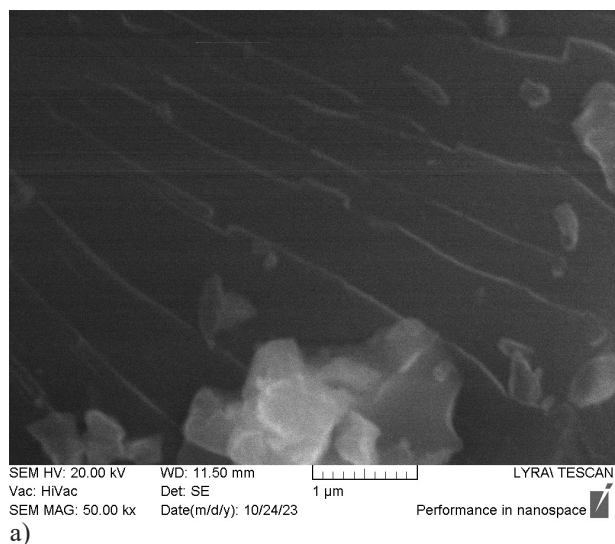
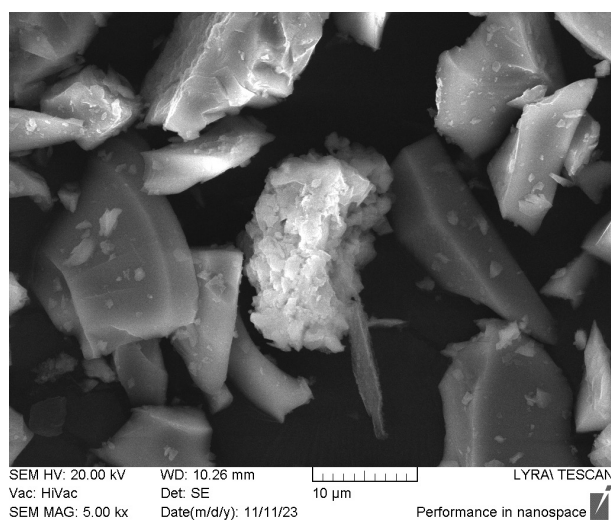
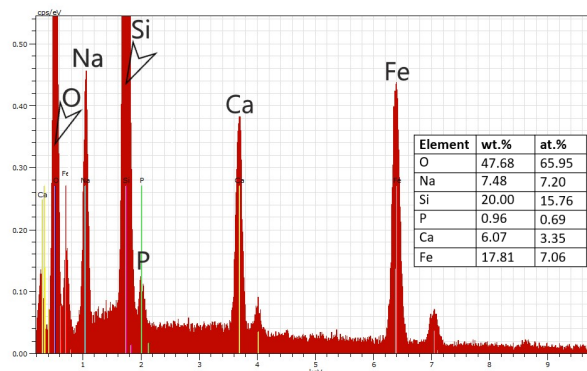


Fig. 5. SEM microphotographs of the surface of the glass samples before and after the performed SBF tests: (a) untreated glass with 5 mol % Fe_2O_3 ; (b) the same sample after immersion in SBF for 4 days; (c) 7 days; (d) 14 days; (e) 28 days; (f) glass with 5.3 mol % Fe_2O_3 after 28 days in SBF.



g)



h)

Fig. 5. SEM microphotographs of the surface of the glass samples before and after the performed SBF tests: (g) and (h) - glass with 8.1 mol % Fe_2O_3 after 28 days in SBF and corresponding EDX spectrum. - *continued*.

Table 2. Batch chemical composition of the investigated samples and experimentally estimated chemical composition, according to the performed EDX analyses, (wt. %).

Elements	with 5 mol % Fe_2O_3		with 5.3 mol % Fe_2O_3		with 8.1 mol % Fe_2O_3	
	Batch	EDX	Batch	EDX	Batch	EDX
Na	11.32	11.73	11.84	13.77	9.93	9.44
Ca	6.17	6.25	6.45	6.98	5.54	6.60
Si	29.83	28.21	29.01	23.62	27.98	19.80
Fe	8.60	7.49	9.07	9.26	13.29	15.17

not differ significantly in chemical composition from the rest of the sample surface and do not correspond to calcium phosphates, according to the EDX analyses carried out (Fig. 5h).

In Fig. 6 data concerning the changes in the SBF solutions after the contact with the studied glasses for different periods of time - from 4 to 28 days - are shown. With dashed line the change in the concentration of the blank sample (sample of just SBF) with the elapsing time is shown. The experimental data show that in the solution Si ions are present and their concentration increases with the increasing immersion time up to the 28th day after the beginning of the test. However, it becomes clear that the rate of dissolution of the silicon ions decreases with the increasing time of soaking of the glass into

the SBF solution. A tendency towards the decrease of the P concentration in the solution is established and this trend is most well expressed for the glass with 8.1 mol % Fe_2O_3 . A slight increase in the concentration of the Ca ions in the SBF solution is detected during the interaction with the glasses with 5 and 5.1 mol % Fe_2O_3 , while the concentration of Ca ions in the solution for the composition with 8.1 mol % Fe_2O_3 remains lower than that of the initial solution. The performed analyses show neither the presence of Fe nor a significant change in the concentration of Na in the solution.

The measured pH values of the solutions do not show any significant changes. pH values show a slight tendency towards increase from 7.4 to 7.5-7.6 within the whole period of duration of 28 days for the performed tests.

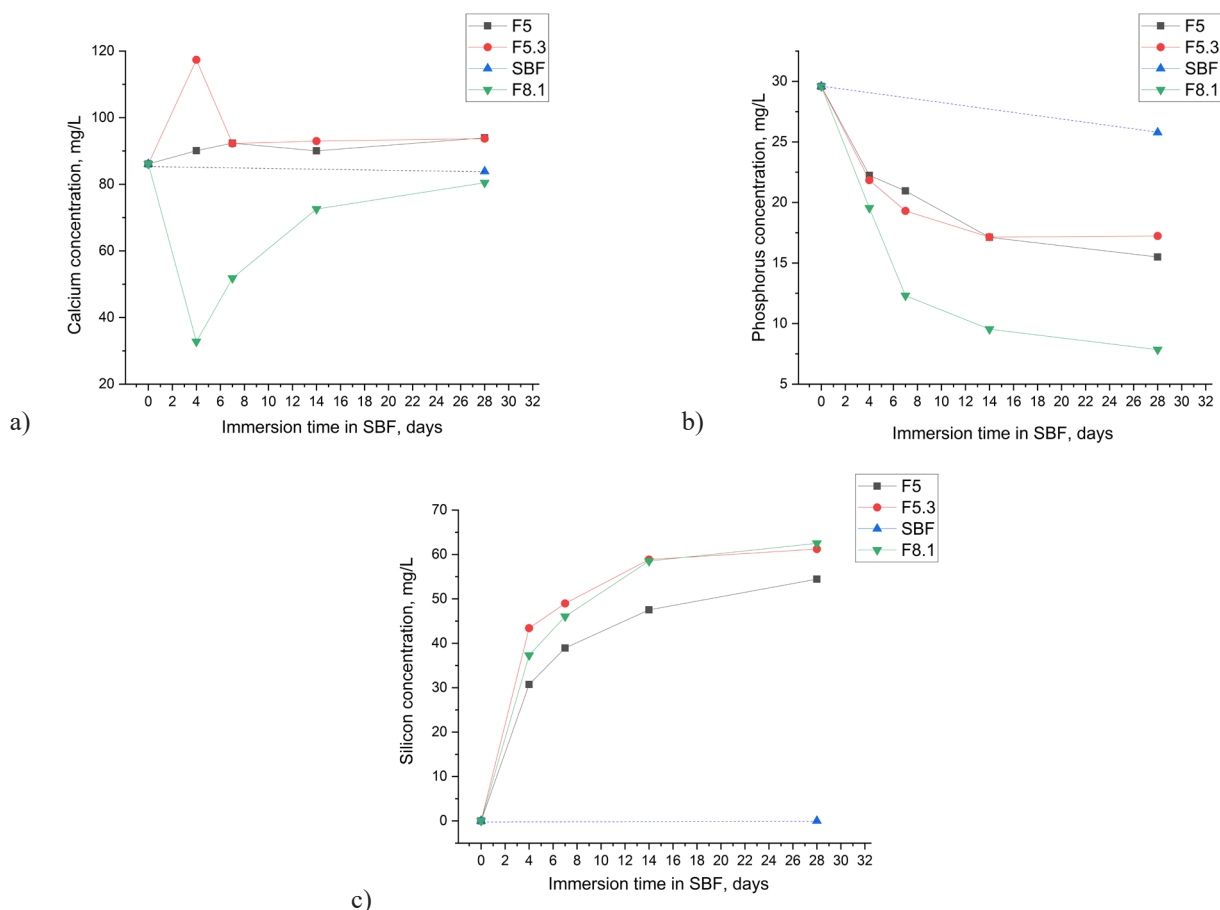


Fig. 6. The values of Ca²⁺ (a), P⁵⁺ (b), Si⁴⁺ (c) concentrations in SBF solution for the immersed glass samples F5 (5 mol % Fe₂O₃), F5.3 (5.3 mol % Fe₂O₃) and F8.1 (8.1 mol % Fe₂O₃) as a function of time.

CONCLUSIONS

Three soda lime silicate glasses containing Fe₂O₃ with concentration between 5 and 8.1 mol % are prepared via the traditional melt-quenching technique and their physico-chemical and structural characterization is performed. The amorphous nature of the prepared materials is confirmed by the XRD and optical microscopy analyses carried out. The data from the FT-IR analyses witnesses that in the glass structure SiO₄ tetrahedra with two bridging and two non-bridging oxygens are prevalingly present. The *in vitro* bioactivity of the samples is studied by immersing them in a SBF. As a result of the performed FT-IR and SEM-EDX analyses on the untreated and SBF treated glasses, it is established that after the 28 days immersion test the glasses do not form an apatite-like layer on the contact surface with the SBF solution, i.e. they do not demonstrate *in vitro*

bioactivity. However, it is proven that the samples interact with the SBF solution, and this leads to certain changes in them which is witnessed by the detected shift in the maxima of the absorption bands attributed to the SiO₄ tetrahedra vibrations. It could be thus concluded that the proposed glasses are only slightly soluble in the SBF, according to the data for the ionic concentration and the pH values of the solutions.

Acknowledgements

The authors express their gratitude to the Research Centre at the University of Chemical Technology and Metallurgy, project № 12279 for the financial support in carrying out the bioactivity tests.

The preparation of the glasses and the structural investigations are financially supported by contract KII-06-H48/4 with the Bulgarian National Science Fund.

REFERENCES

1. E.M. Múzquiz-Ramos, V. Guerrero-Chávez, B.I. Macías-Martínez, C.M. López-Badillo, L.A. García-Cerda, Synthesis and characterization of maghemite nanoparticles for hyperthermia applications, *Ceram. Int.*, 41, 1, 2015, 397-402.
2. S. Palanisamy, Y.M. Wang, Superparamagnetic iron oxide nanoparticulate system: synthesis, targeting, drug delivery and therapy in cancer, *Dalton Trans.* 48, 26, 2019, 9490-9515.
3. X. Wang, A. Deng, W. Cao, Q. Li, L. Wang, J. Zhou, B. Hu, X. Xing, Synthesis of chitosan/poly (ethylene glycol)-modified magnetic nanoparticles for antibiotic delivery and their enhanced anti-biofilm activity in the presence of magnetic field, *J. Mater. Sci.*, 2018, 53, 9, 6433-6449.
4. A. Rayegan, A. Allafchian, I.A. Sarsari, P. Kameli, Synthesis and characterization of basil seed mucilage coated Fe_3O_4 magnetic nanoparticles as a drug carrier for the controlled delivery of cephalexin, *Int. J. Biol. Macromol.* 113, 2018, 317-328.
5. X. Yang, X. Zhou, M. Zhu, D. Xing, Sensitive detection of *Listeria monocytogenes* based on highly efficient enrichment with vancomycin conjugated brush-like magnetic nano-platforms, *Biosens. Bioelectron.*, 91, 2017, 238-245.
6. J. Wang, H. Wu, Y. Yang, R. Yan, Y. Zhao, Y. Wang, A. Chen, S. Shao, P. Jiang, Y.Q. Li, Bacterial species-identifiable magnetic nanosystems for early sepsis diagnosis and extracorporeal photodynamic blood disinfection, *Nanoscale*, 10, 1, 2018, 132-141.
7. H. Shen, J. Wang, H. Liu, L. Zhihao, F.B. Jiang, F. Wang, Q. Yuan, Rapid and selective detection of pathogenic bacteria in bloodstream infections with aptamer-based recognition, *ACS Appl. Mater. Interf.*, 8, 30, 2016, 19371-19378.
8. C. Xu, O.U. Akakuru, J. Zheng and A. Wu, Applications of Iron Oxide-Based Magnetic Nanoparticles in the Diagnosis and Treatment of Bacterial Infections, *Frontiers in Bioengineering and Biotechnology*, 7, 2019, Article 141.
9. P. Bhattacharya, S. Neogi, Gentamicin coated iron oxide nanoparticles as novel antibacterial agents, *Mater. Res. Express* 4, 9, 2017, 095005.
10. K. Zomorodian, H. Veisi, S.M. Mousavi, M.S. Ataabadi, S. Yazdanpanah, J. Bagheri, A.P. Mehr, S. Hemmati, H. Veisi, Modified magnetic nanoparticles by PEG-400-immobilized Ag nanoparticles ($\text{Fe}_3\text{O}_4@$ PEG-Ag) as a core/shell nanocomposite and evaluation of its antimicrobial activity, *Int. J. Nanomed.*, 13, 2018, 3965-3973.
11. S.J. Soenen, M. De Cuyper, Assessing iron oxide nanoparticle toxicity in vitro: current status and future prospects, *Nanomedicine (Lond)*, 5, 8, 2010, 1261-75.
12. S.J. Soenen, M. De Cuyper, S.C. De Smedt, K. Braeckmans, Investigating the toxic effects of iron oxide nanoparticles, *Methods Enzymol.* 509, 2012, 195-224.
13. U.S. Patil, S. Adireddy, A. Jaiswal, S. Mandava, B.R. Lee, D.B. Chrisey, In Vitro/In Vivo Toxicity Evaluation and Quantification of Iron Oxide Nanoparticles, *Int. J. Mol. Sci.*, 16, 10, 2015, 24417-50.
14. U.S. Gaharwar, R. Meena, P. Rajamani, Iron oxide nanoparticles induced cytotoxicity, oxidative stress and DNA damage in lymphocytes, *J. Appl. Toxicol.*, 37, 10, 2017, 1232-1244.
15. M.V. Velasco, M.T. Souza, M.C. Crovace, A.J. Aparecido de Oliveira, E.D. Zanotto, Bioactive magnetic glass-ceramics for cancer treatment, *Biomed. Glasses* 5, 1, 2019, 148-177.
16. T. Kokubo, Y. Ebisawa, Y. Sugimoto, M. Kiyama, K. Ohura, T. Yamamuro, M. Hiraoka, M. Abe, Preparation of bioactive and ferromagnetic glass-ceramic for hyperthermia in: J.E. Hulbert, S.F. Hulbert (Eds.), *Bioceramics*, Vol. 3, Rose-Hulman Institute of Technology, Terre Haute, IN, 1992, pp. 213-223.
17. T. Kokubo, Preparation and properties of composite ceramics for biomedical applications, *J. Japan Soc. Powder Metall.*, 37, 2, 1990, 324-328.
18. Y. Ebisawa, Y. Sugimoto, T. Hayashi, T. Kokubo, K. Ohura, T. Yamamuro. Crystallization of (FeO , Fe_2O_3)-CaO - SiO_2 glasses and magnetic properties of their crystallized products, *J. Ceram. Soc. Japan.*, 99, 1, 1991, 7-13.
19. Y. Ebisawa, T. Kokubo, K. Ohura and T. Yamamuro, Bioactivity of Fe_2O_3 -containing CaO - SiO_2 glasses: in vitro evaluation, *J. Mater. Sci., Mater. Med.*, 4, 1992, 225-232.
20. W. Luo, B. Li, Y. Wang, G. Pan, H. Wu, Synthesis of multifunctional hollow SiO_2 - CaO - Fe_2O_3 glass-ceramic nanospheres, *Int. J. Appl. Ceram. Technol.* 17, 4, 2020, 1843-1851.

21. Y.Y. Wang, B. Li, W.Q. Luo, F. Cao, Bioactivity of Fe_2O_3 - CaO - SiO_2 glass ceramics modified through the addition of P_2O_5 and TiO_2 , *Ceram. Int.* 43, 9, 2017, 6738-6745.
22. R.K. Singh, G.P. Kothiyal, A. Srinivasan, Magnetic and structural properties of CaO- SiO_2 - P_2O_5 - Na_2O - Fe_2O_3 glass ceramics, *J. Magn. Magn. Mater.*, 320, 7, 2008, 1352-1356.
23. P. Ji, Y. Wang, M. Zhang, B. Li, G. Zhang, P_2O_5 - Fe_2O_3 - CaO - SiO_2 ferromagnetic glass-ceramics for hyperthermia, *Int. J. Appl. Ceram. Technol.*, 15, 5, 2018, 1261-1267.
24. M. Abbasi, B. Hashemi, H. Shokrollahi, Investigating in vitro bioactivity and magnetic properties of the ferrimagnetic bioactive glass-ceramic fabricated using soda-lime-silica waste glass, *J. Magn. Magn. Mater.*, 356, 2014, 5-11.
25. R.K. Singh, A. Srinivasan, G.P. Kothiyal, Evaluation of CaO - SiO_2 - P_2O_5 - Na_2O - Fe_2O_3 bioglass-ceramics for hyperthermia application, *J. Mater. Sci.: Mater. Med.*, 20, 2009, 147-151.
26. S. El Shabrawy, C. Bocker, C. Rüssel, Crystallization of MgFe_2O_4 from a glass in the system $\text{K}_2\text{O}/\text{B}_2\text{O}_3/\text{MgO}/\text{P}_2\text{O}_5/\text{Fe}_2\text{O}_3$, *Solid State Sci.*, 60, 2016, 85-91.
27. O. Bretcanu, M. Miola, C.L. Bianchi, I. Marangi, R. Carbone, I. Corazzari, M. Cannas, E. Vernè, In vitro biocompatibility of a ferromagnetic glass-ceramic for hyperthermia application, *Mater. Sci. Eng. C Mater. Biol. Appl.*, 73, 2017, 778-787.
28. O. Bretcanu, E. Verne, M. Coisson, P. Tiberto, P. Allia, Temperature effect on the magnetic properties of the coprecipitation derived ferrimagnetic glass-ceramics, *J. Magn. Magn Mater.*, 300, 2, 2006 412-417.
29. W. Leenakul, P. Intawin, T. Tunkasiri, J. Ruangsuriya, K. Pengpat, Preparation of ferrimagnetic BF based silicate glass system, *Ceram. Int.*, 41, 2015, S464-S470,
30. S.A. Shah, M. Hashmi, S. Alam, A. Shamim, Magnetic and bioactivity evaluation of ferrimagnetic ZnFe_2O_4 containing glass-ceramics for the hyperthermia treatment of cancer, *J. Magn. Magn Mater.* 322, 3, 2010, 375-381.
31. Y.Y. Wang, B. Li, Y.Y. Wang, Characterization of Fe_2O_3 - CaO - SiO_2 Glass-Ceramics Prepared by Sol-Gel, *Appl. Mech. Mater.*, 624, 2014, 114-118.
32. F. Baino, E. Fiume, M. Miola, F. Leone, B. Onida, F. Laviano, R. Gerbaldo, E. Verne, Fe-doped sol-gel glasses and glass-ceramics for magnetic hyperthermia, *Materials*, 11, 1, 2018, 173.
33. P. Rastgoo Oskoui, M. Rezvani, Structure and magnetic properties of SiO_2 - FeO - CaO - Na_2O bioactive glass-ceramic system for magnetic fluid hyperthermia application, *Heliyon*, 9, 2023, e18519.
34. N. Shankhwar, A. Srinivasan, Evaluation of sol-gel based magnetic 45S5 bioglass and bioglass-ceramics containing iron oxide, *Mater. Sci. Eng. C Mater. Biol. Appl.*, 62, 2016, 190-196.
35. M. Baikousi, S. Agathopoulos, I. Panagiotopoulos, A.D. Georgoulis, M. Louloudi, M. A. Karakassides, Synthesis and characterization of sol-gel derived bioactive CaO - SiO_2 - P_2O_5 glasses containing magnetic nanoparticles, *J. Sol-Gel Sci. Technol.*, 47, 2008, 95-101.
36. Becke line method. In: Manutchehr-Danai M. (eds) *Dictionary of Gems and Gemology*. 3th Ed. Heidelberg, Berlin, Springer, 2009.
37. T. Kokubo, H. Kushitani, S. Sakka, T. Kitsugi, T. Yamamuro, Solutions able to reproduce in vivo surface-structure changes in bioactive glass-ceramic A-W, *J. Biomed. Mater. Res.*, 24, 6, 1990, 721-734.
38. I. Mihailova, R. Harizanova, T. Tasheva, N. Dimova, C. Rüssel, Physicochemical and structural characterization of silicate glasses containing iron oxides, *J. Chem. Technol. Metall.*, 58, 1, 2023, 3-7.
39. V. Dimitrov, Y. Dimitriev, *Structural analysis (spectral methods)*, Sofia, Bulgaria, UCTM Publishing house, 2009, (in Bulgarian).
40. L. Grund Bäck, S. Ali, S. Karlsson, D. Möncke, E.I. Kamitsos, B. Jonson, Mixed alkali/alkaline earth silicate glasses: physical properties and structure by vibrational spectroscopy, *Int. J. Appl. Glass. Sci.*, 10, 3, 2019, 349-362.
41. R. Parmar, R.S. Kundu, R. Punia, N. Kishore, P. Aghamkar, Fe_2O_3 modified physical, structural and optical properties of bismuth silicate glasses, 2013, Article ID 650207.
42. W.R. Taylo, Application of infrared spectroscopy to studies of silicate glass structure: examples from the melilite glasses and the systems $\text{Na}_2\text{O}-\text{SiO}_2$ and $\text{Na}_2\text{O}-\text{Al}_2\text{O}_3-\text{SiO}_2$, *Proc. Indian Acad. Sci. (Earth Planet. Sci.)*, 99, 1990, 99-117.
43. Y. Ebisawa, T. Kokubo, Bioactivity of $\text{CaO}\cdot\text{SiO}_2$ -based glasses: in vitro evaluation, *J. Mater.Sci.: Materials in Medicine*, 1, 1990, 239-244.